Deposition of trace elements from high temperature gases of Satsuma-Iwojima volcano

F. Africano[1], G. Van Rompaey[1], A. Bernard[1], and F. Le Guern[2]

[1]*Geochemistry CP 160/02, University of Brussels, 50 Av. F. Roosevelt, 1050 Brussels, Belgium*
[2]*CNRS, LSCE, Av. De la Terrasse, 91198 Gif/Yvette, France*

The Satsuma-Iwojima volcano has been emitting continuously high temperature (600° to 900°C) gases for at least 800 years. We identified the minerals that form in response to closed-system cooling of these gases and from air-mixing reactions. Major differences compared with the sublimates observed at other volcanoes are the occurrence of wulfenite ($PbMoO_4$) and several mixed chlorides. This is the first report of wulfenite in fumarolic deposits. Thermochemical modeling shows that wulfenite precipitates between 540° and 490°C from a gas with lower sulfur content and/or higher fO_2, and a higher Mo content ($\log fSO_2 = -2.1$, $\log fH_2S = -5$, $\log fO_2 = -18.6$, $\log fH_2MoO_4 = -4.5$, T $= 500°$C) than the previously reported gas composition. The occurrence of abundant K, Pb, Fe, Zn, Rb and Cs mixed chlorides may be promoted by the low S/Cl of the Satsuma-Iwojima high temperature gases. Natural sublimates of metallic elements (molybdenite, wulfenite, anglesite, Tl-Pb and Tl-Bi sulfides, Mo oxides and Pb oxides) are deposited along the fumarolic conduit and on the ground under conditions of variable temperatures and fO_2. The increase in fO_2 due to the mixing of the gases with the atmosphere reduces the volatility of several elements (As, Sn, Na, K and Pb) by promoting their condensation at higher temperatures. As air mixes with volcanic gas in the fumarolic plume, we can expect to find these metals as aerosols.

1. Introduction

Volcanic emissions are one of the major natural sources of metal compounds in the atmosphere (Nriagu, 1989). Satsuma-Iwojima volcano is emitting continuously high temperature gases for over 800 years (Shinohara *et al.*, 1993), acting as an important contributor to the atmospheric injection of metal compounds (Hedenquist, 1995). The flux of several metals (Fe, Sn, Mo, Zn and Pb) to the atmosphere from the high temperature fumaroles of Satsuma-Iwojima volcano was estimated to range from 1 to 10 t/yr by Hedenquist *et al.* (1994).

The subject of this paper is to investigate the transport and deposition of trace elements such as K, Na, Fe, Cu, Zn, As, Rb, Mo, Cd, Sn, Cs and Pb, which concentrations in the high temperature volcanic gases (600–900°C) range from 1 ppb to 15 ppm. During their transport from the magma to the atmosphere, the volcanic gases cool leading to the precipitation of metal-bearing sublimates. Atmospheric O_2 may enter into the fumarolic vent, mixing with the volcanic gases and contributing to the precipitation of oxidized solid phases. The term "sublimates" is used, in this paper, for the minerals which precipitate directly from the gas phase by vapor deposition processes, including those formed after gas-air mixing.

Le Guern and Bernard (1982) and Bernard (1985) developed a method of collecting sublimates that allows the study of metals deposition in high temperature gases without con-

tamination by atmospheric O_2 and reaction with wall rocks. The silica tubes are introduced into the fumarolic vent, allowing the gases to flow through the tube. Sublimation occurs along a temperature gradient and the minerals are separated according to their temperature of deposition. The deposits on the inner walls of the tubes are formed without air contamination and those on the outer walls are formed by the mixing of the gases with air. Analysis of sublimates collected by this method enable us to identify the form and the temperatures of emission of the trace elements to the atmosphere.

We used different approaches to study the transport and deposition of the trace elements: 1) the mineralogy of sublimates, collected using silica tubes, was analyzed by scanning electron microscope (SEM) and X-ray microdiffration; 2) the mineralogy of the natural sublimates collected from the rock surface was studied by the same methods; 3) we applied the computer code GASWORKS (Symonds *et al.*, 1992; Symonds and Reed, 1993), on a system of 16 elements, to model the cooling of the gases and the precipitation of the solid phases during cooling.

2. Sampling and Analytical Methods

Silica tubes were inserted into three fumaroles at Iwodake crater floor in November 1997 (Fig. 1). Temperatures measured at the inlets of these tubes were 850°, 760° and 535°C. We analyzed the deposits on both, the inner and the outer walls of the tubes. In the laboratory, the silica tubes were cut in sections of 6 to 8 cm and each section was split in several fractions. The small quantity of the deposited ma-
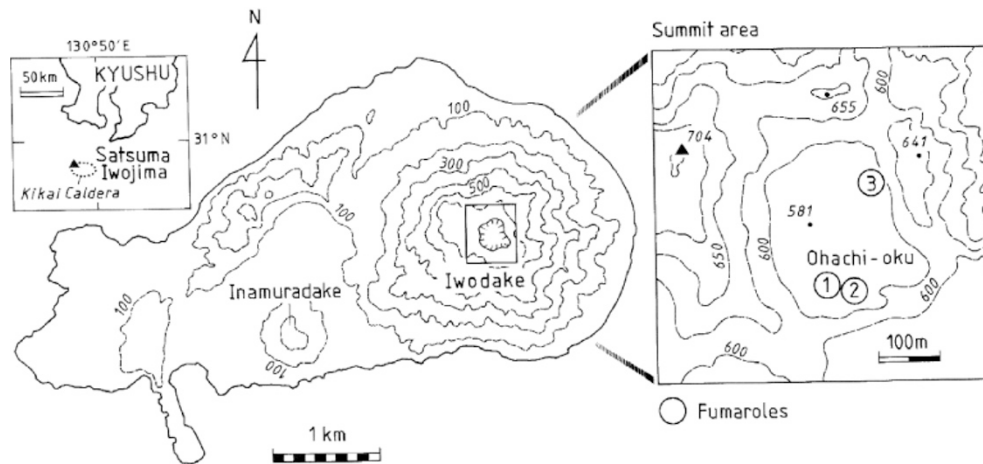
Fig. 1. Map of Satsuma-Iwojima volcano, Iwodake summit crater and location of the sampled high temperature fumaroles.
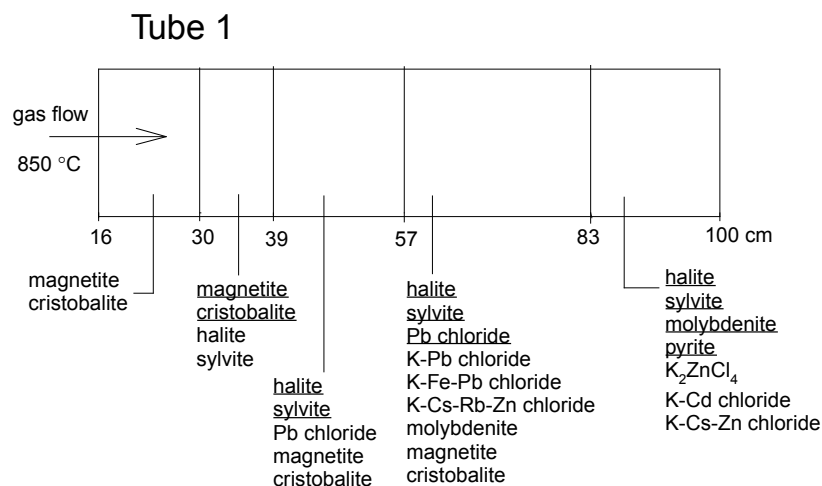

Fig. 2. Assemblages of sublimates precipitated on the inner walls of the silica tube 1. Major phases are underlined. The total amount of minor phases is <10%.

terial (0.5–4.5 mg/cm^2) makes the mineralogical analysis a complex task. Silica tube fragments (1 cm^2) were cut to analyze the deposits directly on the inner and on the outer walls of the tube by SEM and X-ray microdiffraction. The deposits on the tube walls were also scraped and dissolved in pure H$_2$O in order to remove the Na, K chlorides and make the identification of minor phases easier. One aliquot of these insoluble fractions was collected on 0.4 μm Nuclepore filters (Jedwab, 1975) to be analyzed by SEM and optical microscopy and the other aliquot was used for X-ray microdiffraction.

The sublimates, occuring in the walls of ground fissures, were sampled from a few centimeters depth. In the laboratory, we separated natural sublimates from the rock forming minerals based on their morphology. The sublimates are characterized by individual and well-formed crystals deposited on surfaces of fractures.

The sublimates were analyzed with a SEM, JEOL 733 with an energy dispersive X-ray spectrometer (EDS). The EDS detector was equipped with a high X-ray transmission efficiency NORVAR window, which enables detection of the low atomic number elements ($Z > 3$). Chemical composition of minerals was obtained by a standardless procedure using the ZAF matrix correction program. Analyses were carried out at 15 kV and 3 nA.

A BRUKER X-ray microdiffractometer equipped with a new detector GADDS (General Area Detector Diffraction System) was also used to study sublimates mineralogy. Analyses were made at 40 kV and 30 mA with a Cu-K α tube and a graphite monochromator. The GADDS detection system allows the acquisition of X-ray diffraction patterns on very small quantities of powdered materials (5 mg). The X-ray diffraction patterns were obtained with a 500 μm collimator at a working distance of 20 cm and with a resolution of 0.02° 2θ.

3. Mineralogy of the Sublimates
3.1 Silica tubes deposits

Mineral assemblages, separated according to their temperature of deposition, form strips of different colors and

Tube 2   **a**

gas flow

760 °C

20   34   42   63   77   100 cm

magnetite
cristobalite
halite   halite   halite   halite   halite
sylvite   sylvite   sylvite   sylvite   sylvite
ferberite KPb_2Cl_5 KPb_2Cl_5 KPb_2Cl_5 KPb_2Cl_5
pyrite   molybdenite Rb_2ZnCl_4 $KFeCl_3$
molybdenite   pyrite   K-Fe-Rb chloride molybdenite
                ferberite   K-Rb-Cs chloride   molybdenite   wulfenite
                magnetite   K-Zn-Rb chloride   wulfenite   cristobalite
                cristobalite pyrite   cristobalite
                wulfenite   molybdenite   ZnS
                            wulfenite
                            cristobalite

b

gas flow

760°C

20   34   42 cm

cassiterite   cassiterite
cristobalite   aphtitalite
aphtitalite   thenardite
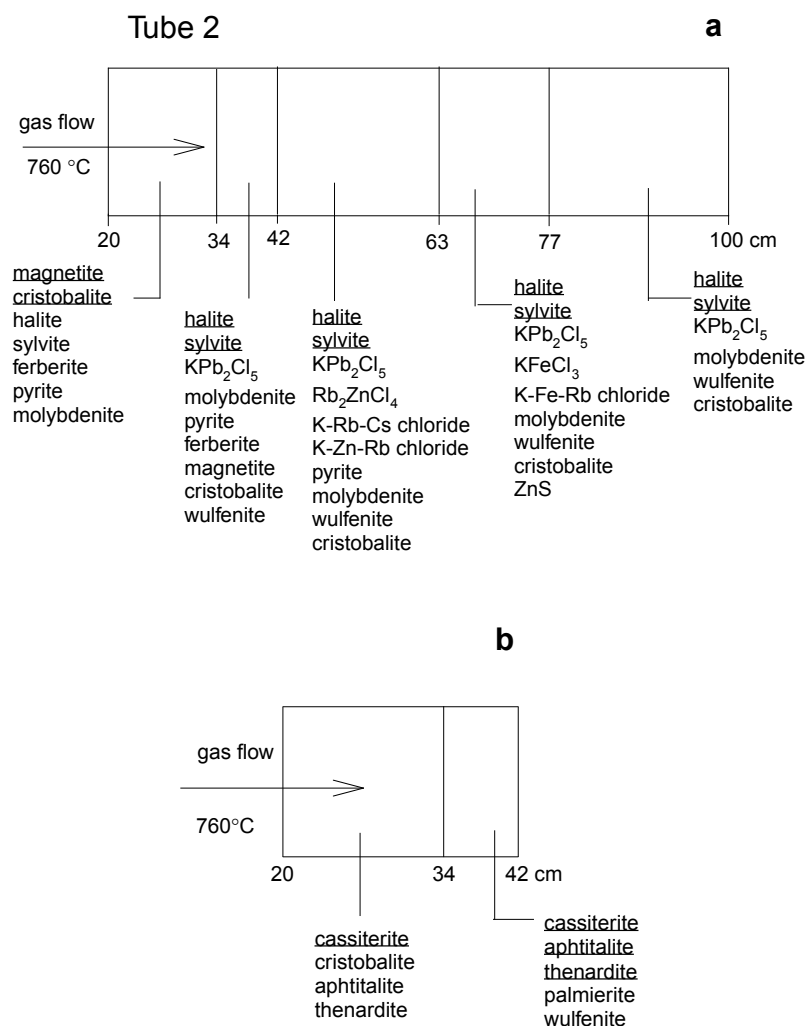thenardite   palmierite
                  wulfenite

Fig. 3. Assemblages of sublimates precipitated on the walls of tube 2. a) inner walls; b) outer walls. Major phases are underlined. The total amount of minor phases is <10%.

widths along the tube walls. The temperature gradient changes along the tube. An important decrease in temperature occurs where the tube is cooled by the atmosphere. To describe the mineralogy of the deposits, we divided the tubes into several zones according to the identified mineral assemblages (Figs. 2, 3 and 4). The minerals identified by SEM and by XRD are presented in Table 1.

3.1.1 Tube 1 (temperature at the inlet = 850°C)

Inner walls

A) 16–30 cm

The deposits are essentially composed of a layer of cryptocristalline magnetite (Fe_3O_4) under a layer of fibrous micron-size cristobalite (SiO_2) which is elongated in the same direction as the gas stream. Dispersed crystals of halite (NaCl) and sylvite (KCl) are also observed (Fig. 5(a)). Sylvite enriched in Br (2 to 6 wt.%) also occurs in aggregates. Bromine is known to replace Cl in sylvite (Coradossi and Mazzi, 1985; Quisefit *et al.*, 1989).

B) 30–39 cm

Cristobalite and magnetite are the predominant phases but their morphology are different from that of the previous zone. Cristobalite occurs as spheres (20–30 μm) and

magnetite occurs as well-formed octahedrons (20–30 μm). Epitaxial overgrowth of cristobalite and magnetite crystals is also observed (Fig. 5(b)). The large size and well-formed crystals suggest deposition from a slightly supersaturated gas.

C) 39–57 cm

Halite and sylvite (Fig. 5(c)) are the dominant phases from here until the end of the tube. Sylvite enriched in Rb (0.5 wt.%) occurs in aggregates. This zone is also marked by the occurrence of a Pb bearing chloride.

D) 57–83 cm

This zone is distinguished by the precipitation of foliated molybdenite (MoS_2, 20–40 μm) which becomes more abundant after 65 cm. Magnetite and cristobalite are rare. The Pb chloride becomes more abundant. Peaks corresponding to cotunnite ($PbCl_2$) were identified in XRD patterns. Unidentified K-Pb and K-Fe-Pb bearing chlorides are frequently observed. Unidentified K-Cs-Rb-Zn chloride which general formula calculated from SEM analyses is $K_{2.1}Cs_{0.3}Rb_{0.9}Zn_{1.3}Cl_6$ is also present.

E) 83–100 cm

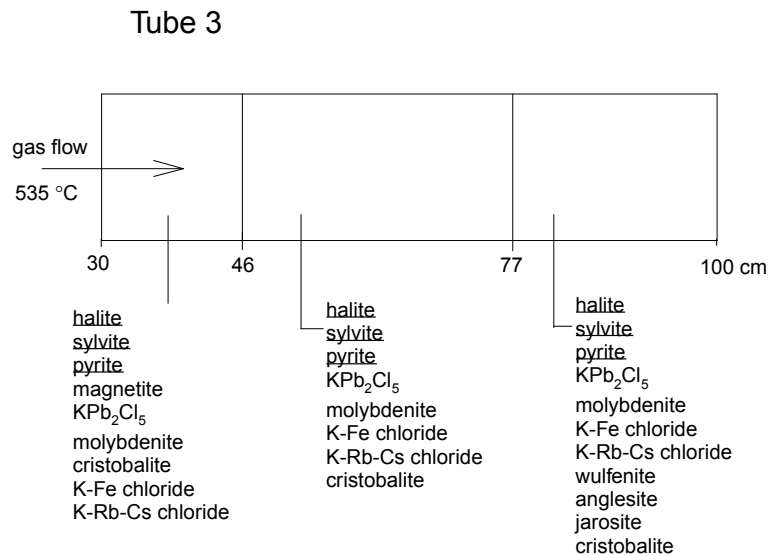Pyrite (FeS_2) coexists with rare magnetite in the first cen-

Tube 3

gas flow

535 °C

30   46   77   100 cm

halite
sylvite
pyrite
magnetite
KPb_2Cl_5
molybdenite
cristobalite
K-Fe chloride
K-Rb-Cs chloride

halite
sylvite
pyrite
KPb_2Cl_5
molybdenite
K-Fe chloride
K-Rb-Cs chloride
cristobalite

halite
sylvite
pyrite
KPb_2Cl_5
molybdenite
K-Fe chloride
K-Rb-Cs chloride
wulfenite
anglesite
jarosite
cristobalite

Fig. 4. Assemblages of sublimates precipitated on the inner walls of the silica tube 3. Major phases are underlined. The total amount of the other phases is <10%.

Table 1. Minerals identified by XRD. The identification was confirmed by SEM and EDS.

Mineral name	Chemical formula	PDF card number
magnetite	Fe_3O_4	19-0629
cristobalite	SiO_2	39-1425
halite	$NaCl$	05-0628
sylvite	KCl	41-1476
aphtitalite	$K_3Na(SO_4)_2$	20-0928
thenardite	Na_2SO_4	37-1465
molybdenite	MoS_2	37-1492
pyrite	FeS_2	42-1340
ferberite	$FeWO_4$	46-1446
wulfenite	$PbMoO_4$	44-1486
anglesite*	$PbSO_4$	36-1461
palmierite	$K_2Pb(SO_4)_2$	29-1015
jarosite	$KFe_3(SO_4)_2(OH)_6$	22-0827
hydroniumjarosite	$(H_3O)Fe_3(SO_4)_2(OH)_6$	31-0650
cassiterite	SnO_2	41-1445
cotunnite	$PbCl_2$	26-1150
synthetic	Rb_2ZnCl_4	30-1100
synthetic	K_2ZnCl_4	33-1060
synthetic	KPb_2Cl_5	27-1364
synthetic	$KFeCl_3$	27-0403
ilsemannite*	$Mo_3O_{8.}xH_2O$	21-0574

*only observed in natural sublimates.
PDF - Powder diffraction file database (JCPDS-International Center for Diffraction Data).

timeters of this zone and become abundant (Fig. 5(d)) at the end of the tube where pyrite and molybdenite compose the insoluble fraction of the deposits. Other K bearing chlorides replace those observed in the previous zone. Unidentified K-Cd and K-Cs-Zn chlorides ($K_{1.6}Cd_{2.3}Cl_6$; $K_{2.3}Cs_{0.5}Zn_{1.5}Cl_6$) are present. A K-Zn chloride is abundant with XRD patterns similar to K_2ZnCl_4.

3.1.2 Tube 2 (temperature at the inlet = 760°C)
Inner walls
A) 20–34 cm
The first deposits occur at 20 cm and are composed of small (5 μm) octahedrons of magnetite and spherical aggre-
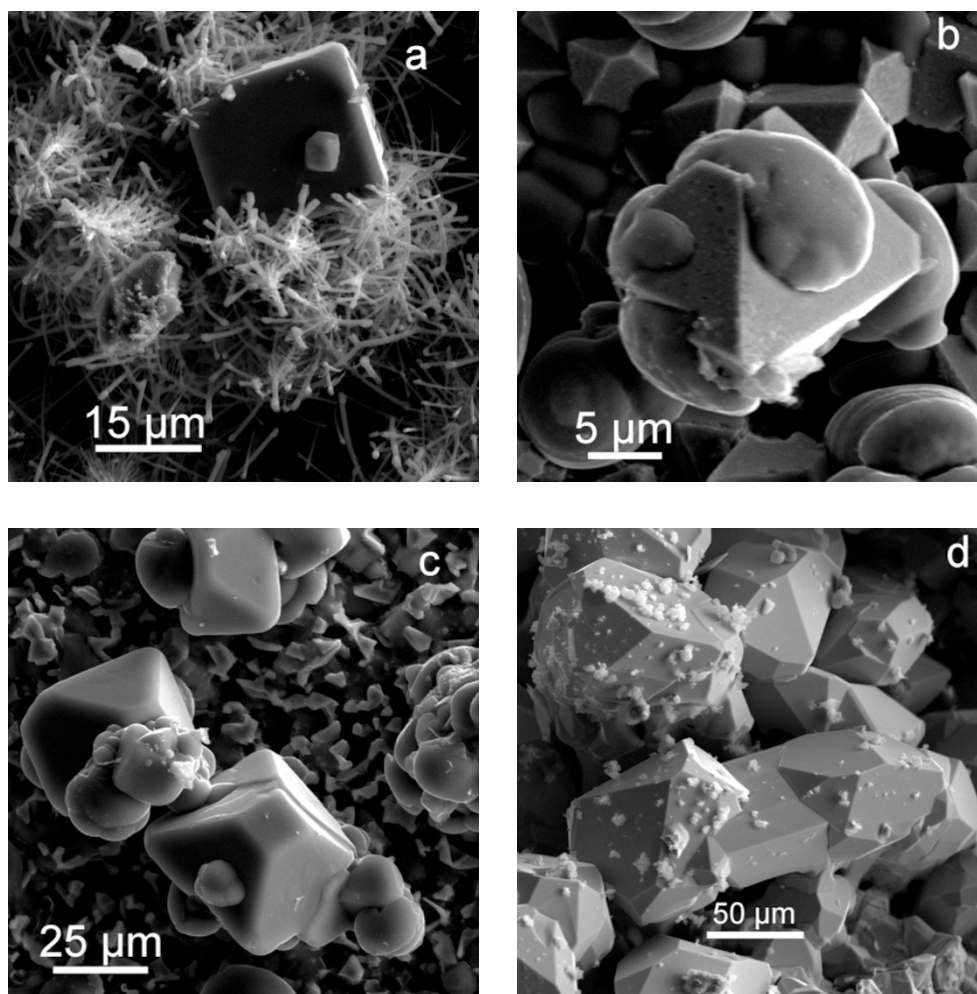
Fig. 5. SEM images of the sublimates inside tube 1. a) cubic crystals of halite mixed with cristobalite in section A; b) intergrow of magnetite and cristobalite crystals in section B; c) octahedrons of sylvite and spheres of cristobalite in section C; d) crystals of pyrite in section E.

gates (10–15 μm) of small (1 μm) crystals of cristobalite. Ferberite (FeWO$_4$) and pyrite are mixed with these oxides. Halite and sylvite are dispersed among the deposits. The halides become more abundant at the end of this zone where molybdenite precipitates. Figures 6(a) and (b) show the XRD patterns of the insoluble fraction and of the bulk deposit of this zone, respectively.

B) 34–42 cm

The halides are the predominant phases till the end of the tube. This zone is distinguished by the precipitation of a K-Pb chloride and wulfenite (PbMoO$_4$, <5 μm) which is only detected on the membrane filters (Fig. 7(a)). This is the first reported occurrence of wulfenite in fumarolic environment. Figures 6(c) and (d) show the XRD patterns of the insoluble fraction and of the bulk deposit of this zone, respectively.

C) 42–63 cm

Ferberite and magnetite disappear in this zone. The K-Pb chloride becomes more abundant and is present till the end of the tube (Fig. 7(b)). Patterns of XRD show the peaks of KPb$_2$Cl$_5$ (Fig. 6(d)) and Rb$_2$ZnCl$_4$ that have been synthetized in the laboratory but never found in nature. Aggregates (60–80 μm) of tabular crystals of unidentified K-Rb-Cs chloride are observed. A K-Zn chloride enriched in

Rb occurs. Pyrite, molybdenite, wulfenite and cristobalite, compose the insoluble fraction with decreasing abundance.

D) 63–77 cm

This zone is marked by the disappearance of pyrite. Iron is incorporated in K-Fe chlorides. Peaks of KFeCl$_3$ are identified in XRD patterns. A K-Fe chloride enriched in Rb (up to 4 wt.%) also occurs. Some isolated crystals of Zn sulfide are observed. Molybdenite, wulfenite and cristobalite occur till the end of the tube.

E) 77–100 cm

Difference with the previous zone is the absence of Fe bearing phases.

Outer walls

The deposits are observed between 20 and 42 cm and are composed by cristobalite, cassiterite (SnO$_2$), which is the predominant phase, aphtitalite [K$_3$Na(SO$_4$)$_2$], thenardite (Na$_2$SO$_4$), palmierite [K$_2$Pb(SO$_4$)$_2$] and wulfenite. Figures 8(a) and (b) show XRD patterns of the insoluble fraction and of the bulk deposit, respectively.

3.1.3 Tube 3 (temperature at the inlet = 535°C)

Inner walls

A) 30–46 cm

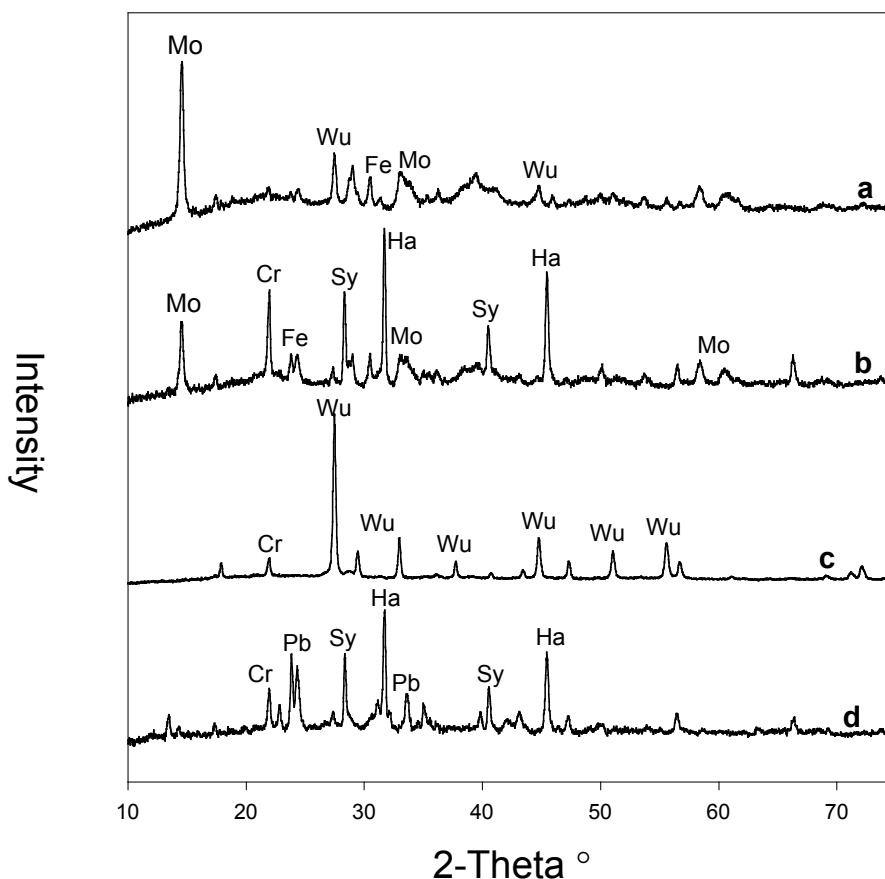First deposition occurs at 30 cm with prevalence of halite

Fig. 6. X-ray microdiffraction patterns of selected samples. a) insoluble fraction from the section A of tube 2; b) bulk deposit from the inner walls of the section A; c) insoluble fraction from the section B of tube 2; d) bulk fraction from the section B. Mineral abbreviations: Cr = cristobalite; Fe = ferberite; Ha = halite; Mo = molybdenite; Pb = synthetic KPb_2Cl_5; Sy = sylvite; Wu = wulfenite.

and sylvite. Pyrite is also abundant and coexists with scarce magnetite. Patterns of XRD also show the peaks of KPb_2Cl_5, molybdenite and cristobalite. Other K bearing chlorides (K-Fe chloride, K-Rb-Cs chloride) are less frequently observed.

B) 46–77cm

The same minerals as in the previous zone occur with exception of magnetite. Cristobalite is also rarely observed.

C) 77–100 cm

In this section of the tube, the same mineral assemblage as in the previous zone is associated with sulfates. Wulfenite, mixed with pyrite, is abundant. Dispersed and well-formed crystals (100–150 μm) of anglesite ($PbSO_4$), jarosite [$KFe_3(SO_4)_2(OH)_6$] and hydroniumjarosite [$(H_3O)Fe_3(SO_4)_2(OH)_6$] occur on the surface of the deposit (Fig. 7(c)).

3.2 Natural sublimates

Minerals deposited on the ground surface are mainly molybdenite (Fig. 7(d)), wulfenite, anglesite, Pb oxide, sulfides of Tl-Pb and Tl-Bi, and Mo oxide (XRD patterns show reflections similar to the hypothetical ilsemannite).

4. Thermochemical Modeling

We used the program GASWORKS (Symonds *et al.*, 1992; Symonds and Reed, 1993) to model: 1) cooling of a high temperature gas of Satsuma-Iwojima fumaroles from 877°C down to 100°C and 2) mixing of the volcanic gas with air and simultaneous cooling. GASWORKS calculates heterogeneous chemical equilibrium among ideal gases, solids and liquids. The thermodynamic database GASTHERM includes more than 1000 gaseous species, solids and liquids for systems with up to 42 elements. We introduced data for wulfenite (Barin, 1993) as this mineral was abundant in tube 2 and was also observed in tube 3. Wulfenite has never been reported in sublimate studies. Symonds *et al.* (1987) and Symonds and Reed (1993) discussed errors in thermochemical data for gaseous $PbCl_4$ and $PbBr_4$. As suggested by these authors, we suppressed $PbCl_4$ and $PbBr_4$ from the database. Lack of thermodynamic data for several phases observed in the tubes, such as K-Pb-Zn-Fe bearing chlorides, is also a limitation of the model as well as the lack of data for Tl, Bi, Cs, Rb, Br and Si concentrations in the volcanic gases. Nevertheless, the modeling results should provide important insights into the natural sublimation process. Calculations were done at 1 bar pressure on a 16-element system (H-C-O-S-Cl-F-N-Na-K-Fe-Zn-Pb-Mo-Cu-As-Sn). We used the chemical composition of the 877°C gas from Iwodake crater (Table 2) in the thermochemical calculations. This composition is similar to the parent gas estimated by Shinohara *et al.* (1993) after correction for CO_2 content (Shinohara *et al.*, 2002). We cooled the gas from 877° to 100°C by 5°C steps. Calculations were done with and without fractionation of
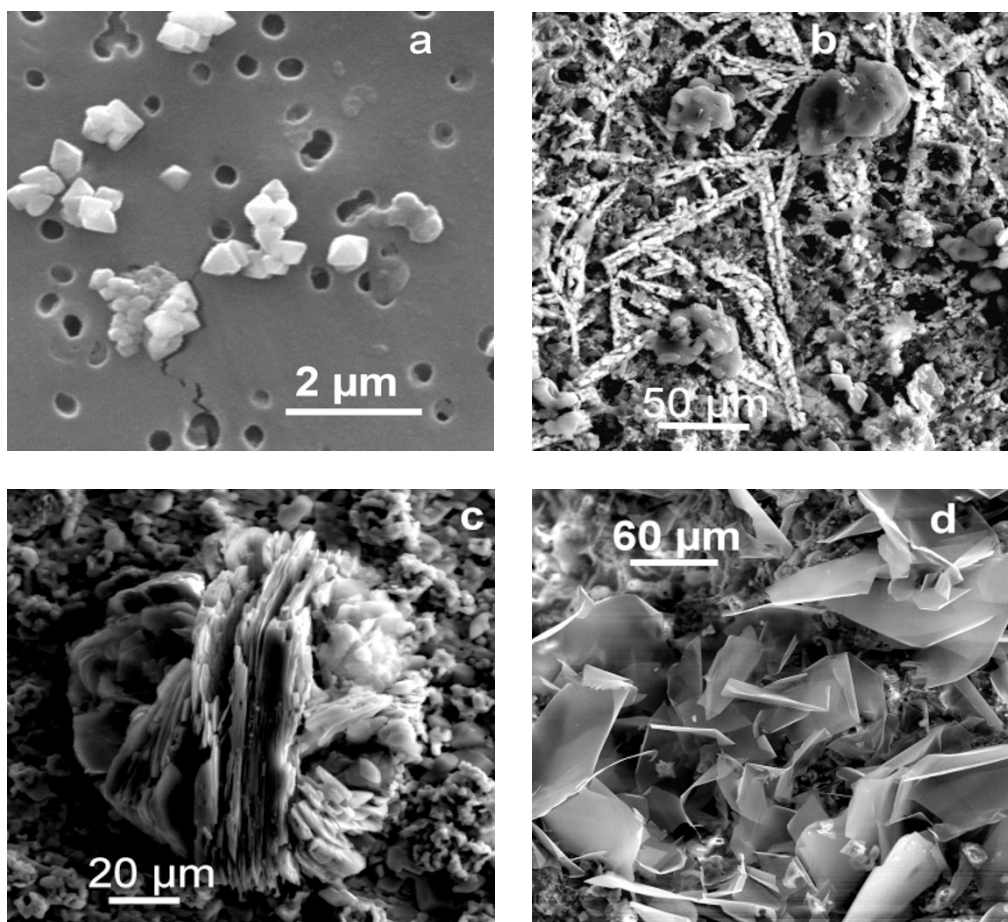
Fig. 7. SEM images of the sublimates. a) crystals of wulfenite inside section B of tube 2, collected on membrane filters; b) prismatic crystals of KPb_2Cl_5 inside section C of tube 2; c) jarosite crystals growing on top of the deposit inside section C of tube 3; d) foliated molybdenite in natural sublimates.
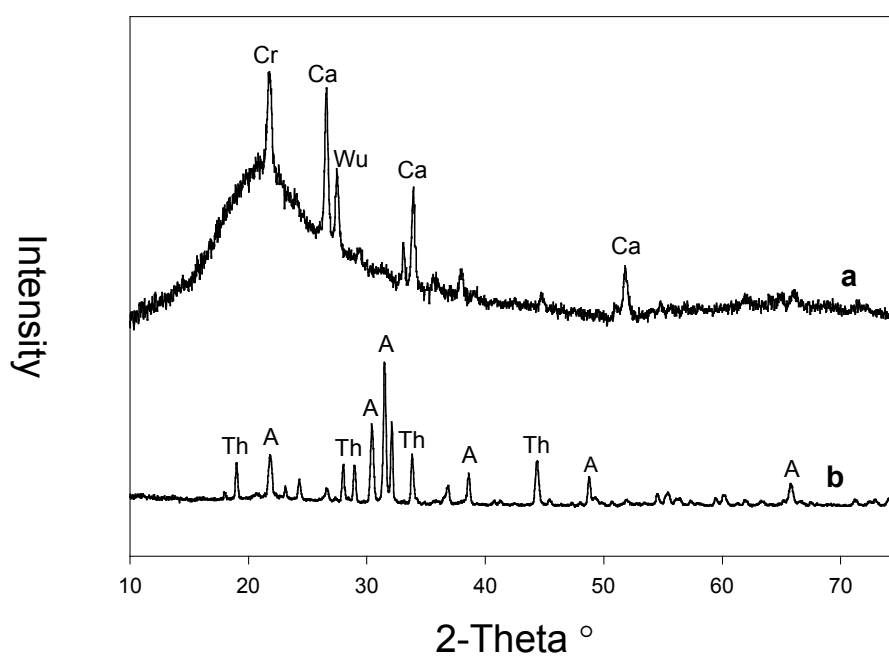

Fig. 8. X-ray microdiffraction patterns of the deposits on the outer walls of tube 2. a) insoluble fraction; b) bulk deposit. Mineral abbreviations: A = Aphthitalite; Ca = cassiterite; Cr = cristobalite; Th = thenardite; Wu = wulfenite.

Table 2. Composition of high temperature fumarolic gases, Iwodake crater, Satsuma-Iwojima volcano (Shinohara *et al.*, 1993; Hedenquist *et al.*, 1994).

T°C	877	702	505
H_2O	97.5	97.61	96.63
CO_2	0.316*	0.341	0.473
St	0.983	1.121	1.058
SO_2	0.918	0.971	0.882
H_2S	0.066	0.149	0.176
HCl	0.677	0.585	1.679
HF	0.033	0.045	0.023
H_2	0.474	0.268	0.132
O_2	<0.001	—	<0.001
N_2	0.008	0.032	0.008
CH_4	0.0003	—	—
CO	0.001	0.0004	0.0005
S/Cl	1.4	1.9	0.63
C/Cl	0.46	0.58	0.28
C/S	0.322	0.30	0.44
	ppm		
Na	12	15	6.1
K	2.10	4.8	1.2
Fe	0.62	1.18	0.06
As	1.74	3.27	4.55
Pb	1.04	1.77	1.27
Zn	0.15	0.24	0.06
Cu	0.03	0.04	0.06
Mo	0.43	0.16	0.03
Sn	0.48	0.78	0.66

Data for major species in mole%.
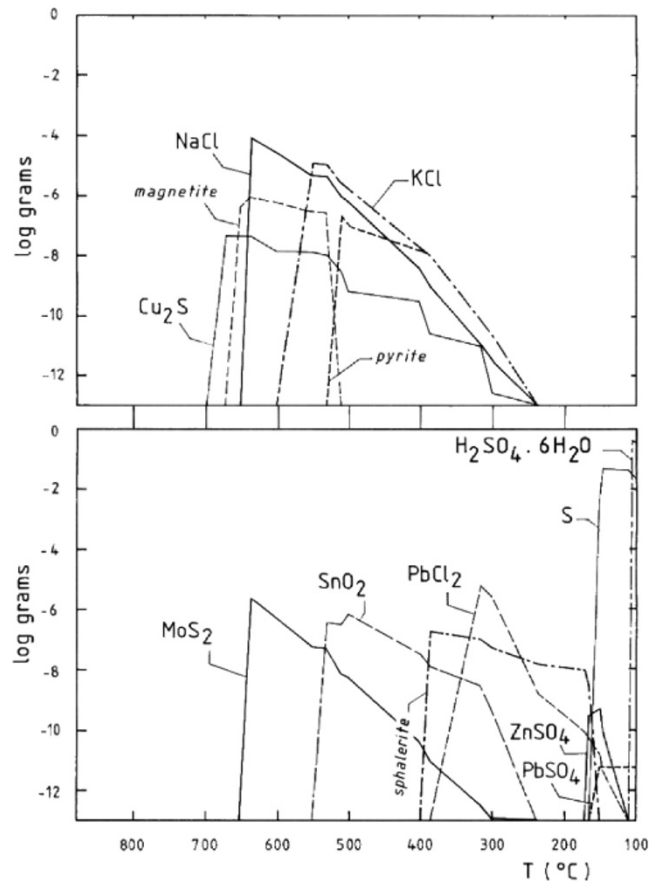*CO_2 values corrected (Shinohara *et al.*, 2002).

Fig. 9. Calculated amounts of solid phases precipitating during cooling of the 877°C gas. The calculations were done under an open system (with fractionation of solids and liquids), without air mixing.

solids and liquids. On calculations with fractionation, the amounts of solids and liquids reaching saturation were removed after each calculation step. We also evaluated the effect of atmospheric oxidation in the precipitation of the solid phases.

4.1   Minerals precipitation during cooling

As the temperature decreases, the metals in a gas phase supersaturate forming mineral assemblages. The calculations with fractionation show that the precipitation of a given phase occurs only in a relatively narrow range of temperature. For each temperature step, the calculated amounts of sublimates are plotted from 877° to 100°C (Fig. 9). Small amounts of Cu_2S precipitate between 700° and 300°C. Magnetite is predominant till 650°C. Halite is the most abundant phase between 650° and 550°C. Sylvite precipitates and becomes predominant at 550°C. Molybdenite is the first sulfide stable (T = 640°C). Precipitation of pyrite occurs from 510° to 400°C. Magnetite completely disappears at 500°C. Cassiterite precipitates from 550° to 240°C. Sphalerite is observed from 400° to 175°C. Cotunnite occurs at temperatures below 325°C. Liquid sulfur forms at 175°C and is

replaced by monoclinic sulfur at 117°C, and $H_2SO_4.6H_2O$ forms at 105°C.

Calculations in the closed system (without fractionation) show the same mineral assemblages within the same temperature ranges with the exception that sulfates (Na_2SO_4, K_2SO_4, $Fe_2(SO_4)_3$, $ZnSO_4$ and $PbSO_4$) replace halides and sulfides at low temperatures (T < 175°C).

4.2   Mixing with air and cooling

We added, in a stepwise manner, small amounts of air (22% O_2 and 78% N_2) to the 877°C gas. Temperature of the mixing air was fixed at 25°C, and the program calculates the temperature of the gas + air mixture at each calculation step. The temperature is calculated as a linear function of the mixture composition, assuming that heat capacities of the volcanic gas and the air are the same (Symonds and Reed, 1993). Temperature decreases from 877° (log fO_2 = −12.1) to 100°C (log fO_2 = −0.7) by addition of 10 moles of air to 1 mole of volcanic gas (Fig. 10(a)). Figure 10(b) shows the mineral assemblages deposited during cooling of the mixture. Hematite precipitates from 850° to 550°C and is replaced by $Fe_2(SO_4)_3$ below 550°C. Cassiterite occurs between 850° and 620°C. Sodium and potassium sulfates are the most abundant phases in this range of temperature. Between 620° and 520°C, $PbSO_4$ is also abundant. Arsenic oxide occurs at temperatures below 600°C. Zinc sulfate precipitates at 520°C. At temperatures below 300°C, MoO_3
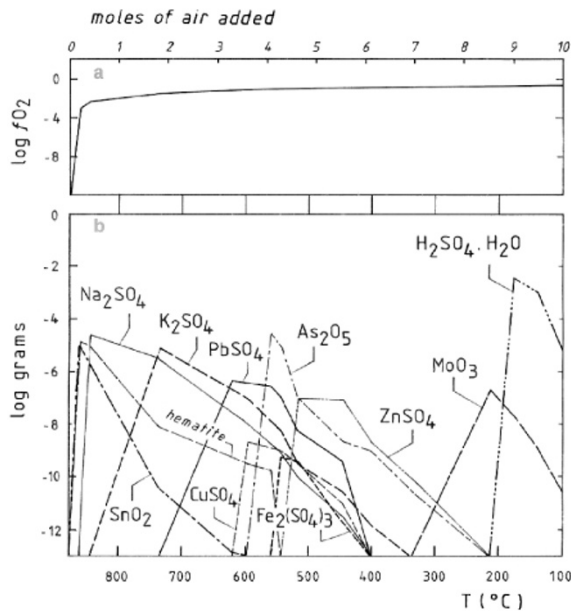
Fig. 10. Thermochemical calculations of gas (877°C)+air (25°C) mixture. The calculations were done under an open system (with fractionation). a) Variation of fO_2 with the amount of air added. Temperature of the mixture decreases according to the mixed amount of air. b) Calculated amounts of solid phases during cooling of the gas + air mixture.

become stable. Hygroscopic sulfuric acid forms at 175°C.

5. Discussion

Before their emission into the atmosphere, a fractionation of the metals from the gas phase occurs by deposition of sublimates along the fumarole conduits. These sublimates, formed under an environment free of air contamination, are typically those observed inside the silica tubes. A fraction of the metals is deposited at the fumarole vents, where atmospheric O_2 may enter. Comparison of the natural sublimates with the results of the thermochemical modeling shows that these minerals were deposited at variable temperature and fO_2 conditions corresponding to different degrees of gas-air mixing. Another fraction of the metals is injected into the atmosphere and condenses in the fumarolic plume as aerosols. These solid phases, formed by the mixing of the gases with the atmosphere, correspond to those observed on the outer walls of the silica tubes.

The mineral assemblages calculated in both thermochemical models of cooling of the high temperature gas and cooling of the gas + air mixture show good agreement with those observed in the inner and the outer walls of the silica tubes. These comparisons allow to constrain the fO_2 conditions and the temperatures of the mineral deposition (Figs. 11(a) and (b)). We assume, in these calculations, an internal equilibrium during the cooling of the gas phase. The prevalence of well-formed crystals in the high temperature zones of the tubes, typical of a slow growing, suggests that they are formed in conditions close to equilibrium. It is also important to note that the rate of oxidation occurring on the outer walls of the tubes seems to be very fast since all the phases observed are typically formed under high fO_2 conditions.
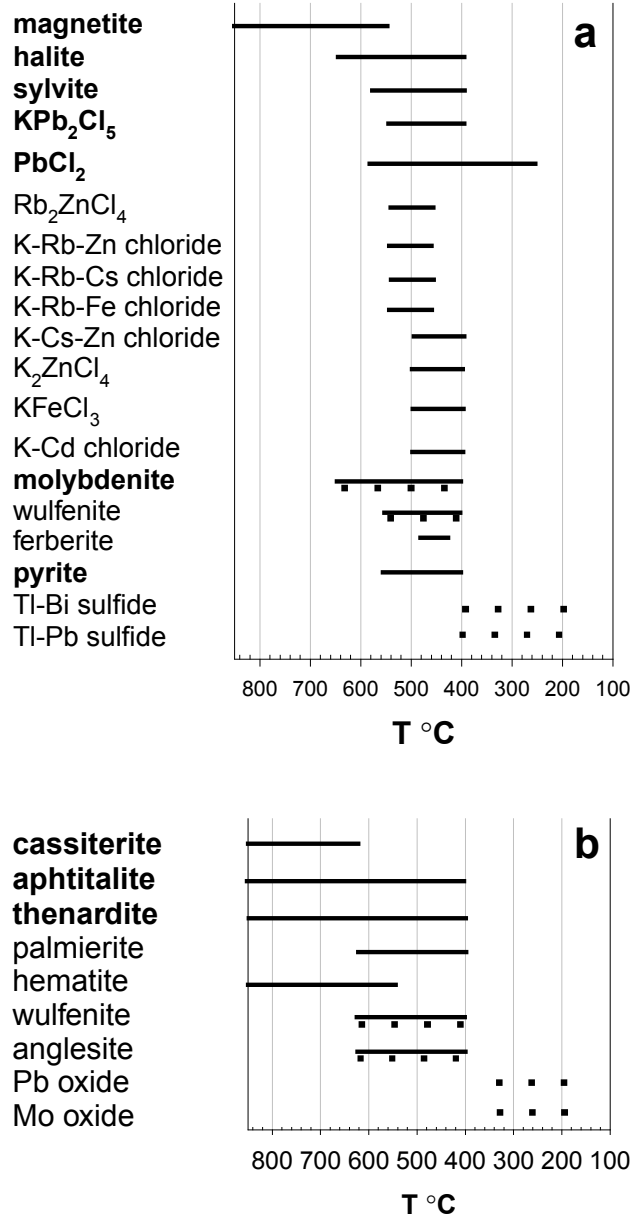
The majority of the sublimates observed in the silica

Fig. 11. Estimated temperature ranges of sublimate deposition. a) Low fO_2 conditions (log $= -12.6$ at 850°C to -28.3 at 300°C). b) High fO_2 conditions (log $= -2.5$ at 850°C to -8.4 at 300°C). The temperatures are estimated on the basis of the thermochemical calculations and/or mineral association in the silica tubes. Solid lines show sublimates observed in the tubes and dotted lines show natural sublimates. Major mineral phases are shown in bold.

tubes are similar with those observed at high temperature fumaroles on other volcanoes situated at subduction zones. Deposition of magnetite at high temperatures (T > 600°C), chlorides at temperatures ranging from 650° to 300°C, molybdenite from 650° to 500°C, ferberite from 600° to 500°C, pyrite from 600° to 300°C are typically reported in high temperature fumaroles with low fO_2 (Bernard, 1985; Symonds *et al.*, 1987; Quisefit *et al.*, 1989). Sulfates are frequently observed inside tubes collected at highly oxidized fumaroles (Bernard, 1985; Taran *et al.*, 2000) or in natural sublimates (Stoiber and Rose, 1974; Naughton *et al.*, 1974; Oskarsson, 1981).

Minerals of highly volatile elements like As, Tl, Se or Sb typically observed in low temperatures (T < 300°C) deposits and in volcanic aerosols (Bernard, 1985; Crowe *et al.*, 1987; Gauthier, 1998) are not observed in the silica tubes analyzed in this study. Temperatures in the tubes studied might be too high to deposit these elements. The calculations show that under high fO_2 (log fO_2 = −1.2) conditions, As condenses at high temperatures (600°C) as As_2O_5. Thallium, which is probably one of the most volatile metals (Gauthier, 1998) is incorporated in Pb and Bi sulfides in natural sublimates.

Wulfenite observed in tubes 2 and 3 and in natural sublimates has never been reported in fumarolic deposits. In low fO_2 conditions, the Pb-bearing solid phases formed are usually galena, Pb-Bi bearing sulfides (Stoiber and Rose, 1974; Bernard, 1985; Symonds *et al.*, 1987; Quisefit *et al.*, 1989) and Pb-bearing chlorides (Symonds *et al.*, 1987; Symonds, 1993; Wahrenberger, 1997). Molybdenum condenses as molybdenite (Stoiber and Rose, 1974; Bernard and Le Guern, 1986; Bernard *et al.*, 1990). In high fO_2 conditions, the Pb sublimates deposited are anglesite (Taran *et al.*, 2000) and palmierite and, at low temperatures, Pb and Mo oxides (Stoiber and Rose, 1974). Wulfenite coexists with halite, sylvite, pyrite and molybdenite in tube 2. Thermochemical modeling shows that this mineral assemblage occurs between 550° and 400°C (Fig. 9). Molybdenum content reported for the Satsuma-Iwojima gases (0.4–1.7 mg/kg; Hedenquist *et al.*, 1994) is similar to those measured in other volcanoes situated at subduction zones. Figure 12 shows the stability of wulfenite, molybdenite and galena, anglesite, and cotunnite with respect to the fugacities of O_2 and S_2 at 500°C. The stability of thenardite and halite is also shown because these phases occur on the outer walls and on the inner walls of the tubes respectively. Compositions of the gases from Satsuma-Iwojima, Merapi and Kudryavy volcanoes, fall in the stability field of molybdenite and halite as observed in tube 1 (Fig. 2). Wulfenite coexists with molybdenite in tube 2 and could be de-
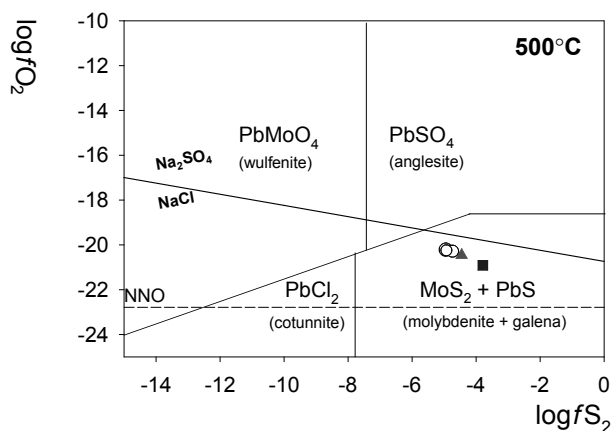
posited from a gas with lower fS_2 and/or with a slightly higher fO_2 than those calculated for the Satsuma-Iwojima gases. We searched the conditions of wulfenite precipitation with GASWORKS by changing H_2S, O_2 and Mo content in the gas. First we cooled the 877°C gas to 500°C (log fO_2 = −20.2; log fSO_2 = −2.1; log fH_2S = −2.6; log fS_2 = −4.9; log fH_2MoO_4 = −7.5). A minimum saturation index for wulfenite (log Q/K = −0.6) is obtained by subtracting 0.2 mol% of H_2S and adding 0.05 mol% of O_2. Wulfenite precipitates by addition of 0.1 mol% of Mo to this gas (log fO_2 = −18.6; log fSO_2 = −2.1; log fH_2S = −5; log fS_2 = −8.2; log fH_2MoO_4 = −4.5), in association with halite, sylvite and molybdenite. The theoretical cooling and heating of this hypothetical 500°C gas show that wulfenite precipitates between 540° and 490°C. These results suggest that the precipitation of wulfenite occurs from a gas with high Mo content. The formation of wulfenite at Satsuma-Iwojima implies that the Mo content of the gases is higher than that reported by Hedenquist *et al.* (1994) and probably higher than those measured at other volcanoes. The abundant Mo bearing minerals in the natural sublimates at Satsuma-Iwojima fumaroles also support this hypothesis.

Lead, Zn, Fe bearing chlorides and mixed K, Cs, Rb, Pb and Zn chlorides have been observed in silica tubes at other sites (Symonds *et al.*, 1987; Symonds, 1993; Wahrenberger, 1997). These chlorides are also abundant in the tubes of Satsuma-Iwojima. Symonds (1993) observed abundant $PbKCl_3$ at temperatures as high as 500°C. Thermochemical calculations with the composition of Merapi high temperature gases show precipitation of galena at T < 400°C replaced by $PbCl_2$ at lower temperatures (Symonds *et al.*, 1987). In the calculation model of the Satsuma-Iwojima gases, the precipitation of galena does not occur which is in agreement with the observations, but $PbCl_2$ precipitates at temperatures (350°C) lower than those of the Pb chlorides occurrence in the tubes. The K, Pb and Zn contents of the gases are similar to those measured at the other sites. The low S/Cl (0.6 to 1.9) of the Satsuma-Iwojima gases explain the stability of the chlorides instead of the sulfides. The incorporation of Rb and Cs in K chlorides, and preferential incorporation of Cs favored by decreasing temperature, were also observed at other sites (Quisefit *et al.*, 1989). Compositional variation of the alkali halides with decreasing temperatures (NaCl > KCl > Rb-Cs bearing chlorides > Cs bearing chlorides) was previously discussed by Symonds and Reed (1993) and agrees with the decreasing volatility within the alkali family (Cs > Rb > K > Na) observed in aerosols (Hinkley *et al.*, 1994; Gauthier, 1998). The calculations show that Na and K precipitate as halides below 650°C in reduced conditions but condense as sulfates at temperatures as high as 850°C from the oxidized gaseous mixture. In silica tubes, Sn is commonly incorporated in Pb-Bi bearing sulfides deposited at temperatures lower than 450°C (Bernard, 1985; Symonds *et al.*, 1987). In the Satsuma-Iwojima tubes, Sn is observed as cassiterite at temperatures from 760°C (temperature of the inlet of the tube 2) to approximately 600°C (minimal calculated temperature of deposition = 620°C) only when the gas mixes with air (log fO_2 = −1.5). The highly oxidized gases of Colima

Fig. 12. Relative stability of wulfenite, anglesite, cotunnite, molybdenite and galena with respect to fO_2 and fS_2. The equilibrium gas compositions were calculated at 500°C with GASWORKS: circles = Satsuma-Iwojima gases, triangle = Kudryavy, 1995 (Fischer *et al.*, 1998), square = Merapi, 1979 (Bernard, 1985). For reference, the Ni/NiO oxygen buffer (NNO) line is also shown by a dashed line.

volcano also deposited cassiterite at temperatures ranging from $550°$ to $800°C$ (Taran *et al.*, 2000). High fO_2 favors the precipitation at higher temperatures of some elements (As, Sn, Na, K and Pb). As air mixes with volcanic gas in the fumarolic plume, we can expect to find these metals as aerosols. The gas-particle conversion may occur in the plume depending on the temperature of the fumarolic emissions.

The occurrence of sulfates at the end of tube 3 suggests that secondary processes occurred after the deposition of the minerals. The larger size of the jarosite crystals and their euhedral morphology suggests that they did not precipitate directly from the supersaturated gaseous phase as the other solid phases. If the gas mixes with air which is allowed to enter in the tube at the extremity, the high fO_2 will result in the formation of hygroscopic H_2SO_4 droplets at low temperatures ($175°C$; Fig. 10; Symonds *et al.*, 1992). The well developed crystals of anglesite and jarosite may be formed by reaction of H_2SO_4 with pyrite and K_2PbCl_5. Cristobalite is observed inside the Satsuma-Iwojima tubes. The formation of this phase in tubes was discussed previously (Bernard, 1985; Symonds *et al.*, 1992) and is due to a volatilization of silica from the tube walls, followed by reprecipitation at lower temperatures.

6.   Concluding Remarks

The results of this study bring information on the temperature and redox conditions at which the gas-to-particle conversion of metals may occur in the Satsuma-Iwojima fumarolic plume. The comparison between the thermochemical models and the mineralogical studies of the silica tubes show general agreement and also, suggests that higher fO_2 due to the mixing of the gases with air during their injection into the atmosphere reduces significantly the volatility of several trace elements. Arsenic, a highly volatile element which is reported to condense at low temperatures ($T < 250°C$) without gas-air mixing, condenses at around $600°C$ as As_2O_5 when the gas reacts with air. Tin starts to condense around $850°C$ as cassiterite, $300°C$ higher than expected without gas-air mixing. Sodium and K which are known to precipitate as halides below $650°C$, condense as sulfates at temperatures as high as $850°C$ from the oxidized gaseous mixture. Lead is deposited as chloride ($T < 550°C$) without gas-air mixing and precipitates as sulfate at $620°C$ in oxidized conditions. Molybdenum, behaves differently from the other metals and precipitates as sulfide at higher temperatures ($650°C$) in reduced conditions but as wulfenite ($fO_2 = -18.6$, $T = 500°C$) under slightly oxidized conditions. When the gas reacts with air, Mo condenses at $300°C$ as oxide. The formation of wulfenite in silica tubes and on the ground suggests a loss of sulfur from the high temperature gas and/or a slightly higher fO_2 than the parent gas. The occurrence of wulfenite also implies that the Mo content of this fumarolic gas should be higher than the previously reported Mo content in the Satsuma-Iwojima gases. The volatility of Fe does not seem to be affected by the fO_2 changes. This metal condenses at temperatures as high as $800°C$ as magnetite or hematite at low and high fO_2 conditions, respectively. The low S/Cl of the Satsuma high temperature gases explain the large abundance of the mixed

chlorides observed. Furthermore, the decreasing temperatures of deposition of the alkali halides (NaCl > KCl > Rb-Cs-bearing chlorides > Cs-bearing chlorides) confirms that, within the alkali family, volatility increases with atomic number (Symonds and Reed, 1993; Hinkley *et al.*, 1994; Gauthier, 1998).

The form in which the trace metals occur in the aerosols will control their behavior in the atmosphere, time of residence, solubility in clouds and final removal in rain or by dry deposition. Previous aerosol studies identified some of the metal bearing phases (Cadle *et al.*, 1979; Rose *et al.*, 1982; Hobbs *et al.*, 1982; Mackinnon *et al.*, 1984; Varekamp *et al.*, 1986; Symonds and Reed, 1993; Toutain *et al.*, 1995; Galindo *et al.*, 1998) but could not provide information on the temperatures or conditions of the aerosols formation. Other solid phases probably present in the plumes might not be identified in the collected aerosols because of their low concentration or because of the small size of the particles (<1 μm). The silica tube method is actually the only way to obtain these data for the volcanic emissions.

References

Barin, I., F. Sauert, and F. Hampson, Thermochemical data of pure substances, 921 pp., VCH, Weinheim, 1993.

Bernard, A., Les mécanismes de condensation des gaz volcaniques (chimie, minéralogie et équilibres des phases condensées majeures et mineures), Thèse de doctorat, Université Libre de Bruxelles, 1985.

Bernard, A. and F. Le Guern, Condensation of volatile elements in high temperature gases of Mt. St. Helens, *J. Volcanol. Geotherm. Res.*, **28**, 91–105, 1986.

Bernard, A., R. Symonds, and W. Rose, Jr., Volatile transport and deposition of Mo, W and Re in high temperature magmatic fluids, *Appl. Geochem.*, **5**, 317–326, 1990.

Cadle, R. D., A. L. Lazrus, B. J. Huebert, L. E. Heidt, W. I. Rose, Jr., D. C. Woods, R. L. Chuan, R. E. Stoiber, D. B. Smith, and R. A. Zielinski, Atmospheric implications of studies of Central American volcanic eruption clouds, *J. Geophys. Res.*, **84**, 6961–6968, 1979.

Coradossi, N. and F. Mazzi, Variazione della constante reticolare a_o con il contenuto di bromo nel chloruro di ammonio naturale (salmiak) di Vulcano (Isole Eolie), *Rend. Soc. Ital. Min. petr.*, **40**, 267–275, 1985.

Crowe, B., D. Finnegan, W. Zoller, and W. Boynton, Trace element geochemistry of volcanic gases and particles from 1983–1984 eruptive episodes of Kilauea Volcano, *J. Geophys. Res.*, **92**, 13708–13714, 1987.

Fischer, T., W. Giggenbach, Y. Sano, and S. Williams, Fluxes and sources of volatiles discharged from Kudryavy, a subduction zone volcano, Kurile Islands, *Earth Planet. Sci. Lett.*, **160**, 81–96, 1998.

Galindo, I., L. Ivlev, A. González, and R. Ayala, Airborne measurements of particle and gas emissions from the December 1994–January 1995 eruption of Popocatépetl volcano (Mexico), *J. Volcanol. Geotherm. Res.*, **83**, 197–217, 1998.

Gauthier, P. J., Nucléides de courtes périodes dans les gaz et les magmas: Contribution à l'Etude du dégazage et de la dynamique des réservoirs magmatiques, Thèse de doctorat, Université Blaise Pascale, Clermont-Ferrand, 1998.

Hedenquist, J. W., The ascent of magmatic fluid: discharge versus mineralization, in *Magmas, Fluids and Ore Deposits: Mineralogical Association of Canada, Short Course*, edited by J. F. H. Thompson, **23**, 263–289, 1995.

Hedenquist, J. W., M. Aoki, and H. Shinohara, Flux of volatiles and ore-forming metals from the magmatic-hydrothermal system of Satsuma Iwojima volcano, *Geology*, **22**, 585–588, 1994.

Hinkley, T. K., M.-F. Le Cloarec, and G. Lambert, Fractionation of families of major, minor, and trace metals across the melt-vapor interface in volcanic exhalations, *Geochim. Cosmochim. Acta*, **58**, 3255–3263, 1994.

Hobbs, P., J. Tuell, D. Hegg, L. Radke, and M. Eltgroth, Particles and gases in the emissions from the 1980–1981 volcanic eruptions of Mt. St. Helens, *J. Geophys. Res.*, **87**, 11062–11086, 1982.

Jedwab, J., A method of extraction and analysis of possible cosmic particles from manganese nodules, *Meteorics*, **10**, 233–240, 1975.

Le Guern, F. and A. Bernard, A new method for sampling and analyzing

volcanic sublimates. Application to Merapi Volcano, Java, *J. Volcanol. Geotherm. Res.*, **12**, 133–146, 1982.

Mackinnon, I., J. Gooding, D. McKay, and U. Clanton, The El Chichón stratospheric cloud: solid particulates and settling rates, *J. Volcanol. Geotherm. Res.*, **23**, 125–145, 1984.

Naughton, J., V. Lewis, D. Hammond, and D. Nishimoto, The chemistry of sublimates collected directly from lava fountains at Kilauea Volcano, Hawaii, *Geochim. Cosmochim. Acta*, **38**, 1679–1690, 1974.

Nriagu, J. O., A global assessment of natural sources of atmospheric trace metals, *Nature*, **338**, 47–49, 1989.

Oskarsson, N., The chemistry of Icelandic lava incrustations and the latest stages of degassing, *J. Volcanol. Geotherm. Res.*, **10**, 93–111, 1981.

Quisefit, J. P., J. P. Toutain, G. Bergametti, M. Javoy, B. Cheynet, and A. Person, Evolution versus cooling of gaseous volcanic emissions from Momotombo Volcano, Nicaragua: Thermochemical model and observations, *Geochim. Cosmochim. Acta*, **53**, 2591–2608, 1989.

Rose, W. I., R. L. Chuan, and D. C. Woods, Small particles in plumes of Mount St. Helens, *J. Geophys. Res.*, **87**, 4956–4962, 1982.

Shinohara, H., W. F. Giggenbach, K. Kazahaya, and J. W. Hedenquist, Geochemistry of volcanic gases and hot springs of Satsuma-Iwojima, Japan: Following Matsuo, *Geochem. J.*, **27**, 271–285, 1993.

Shinohara, H., K. Kazahaya, G. Saito, N. Matsushima, and Y. Kawanabe, Degassing activity from Iwodake rhyolitic cone, Satsuma-Iwojima volcano, Japan: Formation of a new degassing vent, 1990–1999, *Earth Planets Space*, **54**, this issue, 175–185, 2002.

Stoiber, R. E. and W. I. Rose, Jr., Fumarole incrustations at active Central American volcanoes, *Geochim. Cosmochim. Acta*, **38**, 495–516, 1974.

Symonds, R. B., Scanning electron microscope observations of sublimates from Merapi volcano, Indonesia, *Geochem. J.*, **26**, 341–354, 1993.

Symonds, R. B. and M. H. Reed, Calculation of multicomponent chemical equilibria in gas-solid-liquid systems: calculation methods, thermochemical data, and applications to studies of high-temperature volcanic gases with examples from Mount St. Helens, *Amer. J. Sci.*, **293**, 758–864, 1993.

Symonds, R. B., W. I. Rose, M. H. Reed, F. E. Lichte, and D. L. Finnegan, Volatilization, transport and sublimation of metallic and non-metallic elements in high temperature gases at Merapi Volcano, Indonesia, *Geochim. Cosmochim. Acta*, **51**, 2083–2101, 1987.

Symonds, R. B., M. H. Reed, and W. I. Rose, Origin, specification, and fluxes of trace-element gases at Augustine volcano, Alaska: insights into magma degassing and fumarolic processes, *Geochim. Cosmochim. Acta*, **56**, 633–657, 1992.

Taran, Y. A., A. Bernard, J. C. Gavilanes, and F. Africano, Native gold in mineral precipitates from high-temperature volcanic gases of Colima volcano, Mexico, *Appl. Geochem.*, **15**, 337–346, 2000.

Toutain, J. P., J. P. Quisefit, P. Briole, P. Aloupogiannis, P. Blanc, and G. Robaye, Mineralogy and chemistry of solid aerosols emitted from Mount Etna, *Geochem. J.*, **29**, 163–173, 1995.

Varekamp, J. C., E. Thomas, M. Germani, and P. R. Buseck, Particle geochemistry of volcanic plumes of Etna and Mount St. Helens, *J. Geophys. Res.*, **91**, 12233–12248, 1986.

Wahrenberger, C. M., Some aspects of the chemistry of volcanic gases, Dissertation for the degree of Doctor of Natural Science, Swiss Federal Institute of Technology, Zurich, 1997.

F. Africano (e-mail: fafrican@ulb.ac.be), G. Van Rompaey, A. Bernard, and F. Le Guern